

# Operation Stability Enhancement in Once-Through Micro Evaporators

Cor M. Rops, Giaco J. Oosterbaan, Cees W.M. v/d Geld

**Abstract**—Equipment miniaturisation offers several opportunities such as an increased surface-to-volume ratio and higher heat transfer coefficients. However, moving towards small-diameter channels demands extra attention to fouling, reliability and stable operation of the system. The present investigation explores possibilities to enhance the stability of the once-through micro evaporator by reducing its flow boiling induced pressure fluctuations.

Experimental comparison shows that the measured reduction factor approaches a theoretically derived value. Pressure fluctuations are reduced by a factor of ten in the solid conical channel and a factor of 15 in the porous conical channel. This presumably leads to less backflow and therefore to a better flow control.

**Keywords**—Flow boiling, Operation stability, Microfluidics, Microchannels.

## I. INTRODUCTION

**D**URING the last decades fascinating progress has been made in the miniaturisation of micro evaporators. Decreasing the channel diameter leads to an increased surface-to-volume ratio and higher heat transfer coefficients. Additionally, miniaturisation leads to disposable and/or light weight equipment. Recent evaporator designs contain a large number of mini and micro flow channels for evaporating fluids.

However, moving towards small-diameter channels demands extra attention to fouling, reliability and thermo-mechanical management of the system. Apart from that, physical processes limit the maximum achievable heat flux. For instance, if the size is reduced, the pressure drop over a micro channel increases rapidly. Also, the reduced importance of body forces (like gravity and inertia) compared to surface forces (e.g. surface tension) causes an increased probability of channel blockage by the creation of vapour [1]. In once-through micro evaporators, explosive vapour bubble growth is observed [2] and modelled analytically [1]. In case of boiling heat transfer researchers report large pressure fluctuations [3], flow instabilities [4], as well as possible backflow into the divider manifold [5].

Brutin and Tadrist [6], [7] measure the pressure variations over a boiling mini-channel. In their analysis on pressure drop instabilities they found an influence of the inlet condition

(either completely rigid, or with a flexible expansion volume, the flow rate and the heat flux. In case of a connected compressible buffer tank they measure that the outlet pressure exceeds the inlet pressure at certain times during the unstable flow boiling. These instabilities in a boiling minichannel do not comply with the Ledinegg criterion, [8]. Such instabilities are obviously undesirable and need to be overcome.

In-depth investigations and modelling were performed concerning boiling stability in porous media. More than two decades ago Ramesh and Torrance [9], [10] investigated the boiling stability inside a boiling porous medium applying a detailed model for liquid dominated reservoirs based on natural convection. A linear stability study explained the experimental data as shown by Stemmelen et al. [11]. Sahli et al. [12] simplified and extended the model of Ramesh to a more generic two phase stability model. Literature concerning boiling on top of a porous medium is less abundant. Generally, the porous medium is regarded as a micro structured wall influencing the nucleate boiling properties [13], [14]. No literature has been found on boiling on a porous medium through which a gas is blown to lift the liquid from the wall.

The present investigation explores possibilities to enhance the stability of the once-through micro evaporator by reducing its flow boiling induced pressure fluctuations. First, the pressure fluctuations are linked to the total pressure drop. The reduction of the momentum pressure drop is explored first. Widening the channel, and thus creating space for expansion, is found to have much potential. Next, a possible reduction of the frictional pressure drop is examined. It is attempted to lift the boiling liquid from the wall creating an inverted annular flow. An experimental setup, with several test sections, is made to examine both effects, described in section III. In section IV the results are given and discussed. Finally, in the last section conclusions are drawn and recommendations are given.

## II. THEORETICAL BACKGROUND

In general three different contributions to the total pressure drop are recognized:

$$\Delta P_{tot} = \Delta P_{static} + \Delta P_{mom} + \Delta P_{fric} \quad (1)$$

where  $\Delta P_{tot}$  is the total pressure drop over the boiling channel,  $\Delta P_{static}$  is the hydrostatic pressure drop induced by a height difference,  $\Delta P_{mom}$  is the momentum pressure drop generated by the acceleration of the fluid, and  $\Delta P_{fric}$  is the frictional pressure drop. If the slip velocity, i.e. the ratio of the mean gas

C.M. Rops is with the Netherlands Organisation for Applied Scientific Research TNO, 5612 AP Eindhoven, The Netherlands (phone: +31 (0)88 866 63 35; e-mail: cor.rops@tno.nl).

G.J. Oosterbaan is with Eindhoven University of Technology, 5600 MB Eindhoven, The Netherlands (e-mail: g.j.oosterbaan@tue.nl).

C.W.M. v/d Geld is with Eindhoven University of Technology, 5600 MB Eindhoven, The Netherlands (e-mail: c.w.m.v.d.geld@tue.nl).

velocity to the mean liquid velocity inside the channel, is known at each axial position, the first two pressure drops are straightforward to be estimated. The frictional component is usually more difficult to be estimated.

Pressure fluctuations during flow boiling in microchannels are usually linked to explosive vapour bubble growth. The large accelerations ( $> 10^3 \text{ m/s}^2$ ) lead to significant inertia forces, adding to the momentum pressure drop. Reduction of the total momentum pressure drop is therefore expected to have a positive impact on the observed pressure fluctuations. The high (mixture) velocities downstream of the explosively growing vapour bubble blocking a substantial part of the channel lead to increased friction. Thus, reduction of the total (wall) friction is expected to have a positive impact on pressure fluctuations as well.

*A. Two-Phase Flow Pressure Drop in Conical Widening Channel*

**1. Momentum Pressure Drop Reduction in a Conical Widening Channel**

Usually a straight channel with a constant diameter is used. However, on progressively widening channel, going further downstream, obviously lowers the momentum pressure drop. With a single-phase liquid flow at the inlet, the momentum pressure drop of a once-through boiling channel becomes for a channel with a constant diameter

$$\Delta P_{mom} = \frac{G_{tot}^2}{2} \left[ \frac{1}{\rho_{gas}} - \frac{1}{\rho_{liq}} \right] \quad (2)$$

In case of a continuously widening channel with an inlet diameter,  $D_i$ , and an outlet diameter,  $D_o = \alpha D_i$ , the momentum pressure drop becomes:

$$\begin{aligned} \Delta P_{mom} &= \left[ \frac{m_{tot}^2}{2\alpha^4 \frac{\pi^2}{16} D_i^4 \rho_{gas}} - \frac{m_{tot}^2}{2\frac{\pi^2}{16} D_i^4 \rho_{liq}} \right] \\ &= \frac{G_{tot,i}^2}{2} \left[ \frac{1}{\alpha^4 \rho_{gas}} - \frac{1}{\rho_{liq}} \right] \end{aligned} \quad (3)$$

where  $m_{tot}$  is the total mass flow rate, in kg/s, through the widening channel and  $\alpha$  is the ratio of the outflow diameter over the inlet diameter. This implies that the momentum pressure drop can be annihilated by a sufficient widening of the channel ( $\alpha = [\rho_{liq}/\rho_{gas}]^{1/4}$ ). This annihilation of the momentum pressure drop can obviously only be achieved by a widening channel.

**2. Friction Pressure Drop Reduction in a Conical Widening Channel**

Various empirical models have been proposed to estimate the two-phase friction pressure drop. However, the general idea is often to calculate a single phase pressure drop and apply some two-phase multiplier to obtain the two-phase frictional pressure drop component. Most of these models are

similar to the Lockhart-Martinelli two-phase pressure drop model with an adapted Martinelli parameter. The typical form of a pressure drop model for a small diameter channel is therefore:

$$\Delta P_{fric} = \Phi_{CorrLiQ}^2 \Delta P_{liq} \quad (4a)$$

$$\Delta P_{liq} = \frac{a}{Re_{liq}} \frac{\Delta l}{D_h} \frac{((1-x)G_{tot})^2}{2\rho_{liq}} \quad (4b)$$

$$\Phi_{CorrLiQ}^2 = 1 + \frac{C}{\chi} + \frac{1}{\chi^2} \quad (4c)$$

$$\chi^2 = \left( \frac{1-x}{x} \right)^{n_1} \left( \frac{\rho_{gas}}{\rho_{liq}} \right)^{n_2} \left( \frac{\mu_{liq}}{\mu_{gas}} \right)^{n_3} \quad (4d)$$

where  $\Phi_{CorrLiQ}$  is the two-phase flow multiplier applied to the liquid pressure drop over the channel length,  $\Delta P_{liq}$ . Next,  $a$  is the numerical value depending on the channel shape,  $Re_{liq}$  is the Reynolds number based on the liquid mass flux (ie.  $(1-x) \cdot G_{tot}$ ),  $\Delta l$  is the length of the channel,  $D_h$  is the (hydraulic) diameter of the channel,  $G_{tot}$  is the total mass flux, in  $\text{kg/m}^2/\text{s}$ ,  $\chi^2$  is the Martinelli parameter and  $C$  is some model dependent constant, just as  $n_1$ ,  $n_2$  and  $n_3$ .

Similarly to the momentum pressure drop, the friction pressure drop is lowered by a continuously widening channel as compared to a channel with the a constant diameter equal to the mean diameter of the widening channel. Equations (4a-d) show the typical channel diameter dependence of the two-phase friction pressure drop. Rearranging these equations yields:

$$\frac{\Delta P}{\Delta l} = \frac{\Phi_{CorrLiQ}^2 a}{\frac{(1-x)^{m_{tot}} D}{\mu_{liq}}} \frac{1}{D} \frac{1}{2\rho_{liq}} \left( \frac{(1-x) \frac{m_{tot}}{D^2}}{D^2} \right)^2 = c(l) \cdot D^{-4} \quad (5)$$

where  $c(l)$  comprises all terms which are assumed to have no dependency on the channel diameter. The constant  $c$  does vary over the length of the channel since the vapour quality changes over the evaporation length. For a conical channel the vapour quality is conveniently approximated by some power fit depending on  $l$ . A similar power fit can be made with the diameter of the conical channel replacing of the axial position  $l$ . The constant  $c(l)$  can then be redefined as:  $c(l) = const \cdot D^b$ . The power  $b$ , most likely between -1 and 1, will influence the currently assumed minus 4th power. However, given the variety and inconsistency of the empirical models at this level, no indirect diameter dependency ( $b=0$ ) is assumed as a first order approximation. The error due to this assumption is estimated and shown as an error bar in Fig. 1. Next, the friction pressure drop over the channel is calculated by the integral over the length of the widening channel. On assuming a linearly changing diameter, as applicable to the geometry tested, the following expression is derived:

$$\Delta P = \text{const} \int_0^L D^{-4} dl = \text{const} \int_0^L \left[ \frac{D_o - D_i}{L} l + D_i \right]^{-4} dl \quad (6)$$

$$= \frac{\text{const} \cdot L}{3(D_o - D_i)} \left[ D_i^{-3} - D_o^{-3} \right]$$

and therefore by using  $D_o = \alpha D_i$ , the first order approximation friction pressure drop can be written as:

$$\Delta P = \frac{\text{const} \cdot L}{D_i^4} \cdot \frac{-1}{3} \left( \frac{1 - \alpha^{-3}}{1 - \alpha} \right) \quad (7)$$

Equation (7) shows that the pressure drop for a widening channel equals the constant diameter (inlet diameter) channel drop multiplied by a reduction factor depending on the ratio of the exit and entry diameter. Increasing this ratio reduces the geometrical compensation term coming from the conical shape, see Fig. 1.

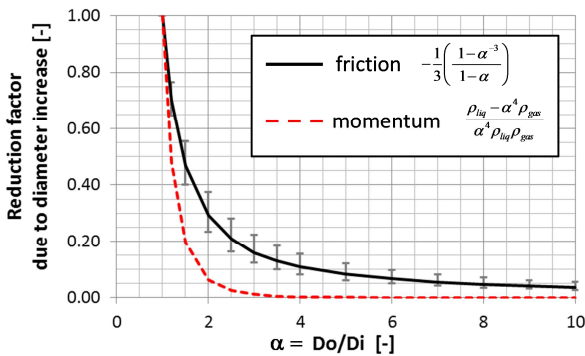


Fig. 1 The factor reducing the friction pressure drop (black solid line) and the momentum pressure drop (red dashed line) over a conical channel compared to a channel with constant diameter equal to the initial diameter of the conical channel.  $D_o$  is the outflow channel diameter,  $D_i$  is the inlet channel diameter.  $\rho_{liq} = 960 \text{ kg/m}^3$ ,  $\rho_{gas} = 0.6 \text{ kg/m}^3$

### B. Active Friction Pressure Drop Reduction

The general idea to estimate the two-phase flow pressure drop is to calculate a single phase liquid pressure drop and apply some two-phase multiplier to obtain the two-phase frictional pressure drop component, see section 2.1. Because of the presence of the gas phase, additional friction inside the liquid must be accounted for. However, applying a gas bearing near the wall is expected to reduce the “single phase” liquid pressure drop, much similar to the reduction of pressure drop in oil transport by the injection of a water layer at the wall [15]. Of course, when adding a gas through the wall the factor “a” in (2b) needs to be adapted.

In industry multiple examples of inverted annular flow can be found. Various researchers have investigated film boiling in heated tubes [16]. However, in literature the main attention goes to the heat transfer from the wall across the thin vapour layer to the liquid. The thickness of the vapour layer determines to a great extent the heat transfer coefficient. The thinner the vapour layer the larger the heat transfer coefficient.

In adiabatic two phase flow the inverted flow pattern occurs. Takamasa et al. [17] observed inverted churn patterns for regular sized pipes (20mm diameter) with a hydrophobic wall. In micro channels a controlled interface can be obtained resulting in stable inverted annular flow. Huh et al. [18] observed that depending on the ratio and the absolute value of the air and water flow various (inverted) types of flow occurred. Detailed stability analyses concerning this topic are available in literature, e.g. [19]. Micro channels have typical perimeters less than  $10^{-2} \text{ m}$ , thus smaller than the typical Taylor wavelength obtained by the Kelvin-Helmholtz instability analysis. This too points in the direction that in micro channels inverted annular flow is not an “unusual” flow pattern.

However, the two phase pressure drop in these inverted systems has not given much attention, nor experimentally nor analytically. To our knowledge no proper models to estimate the two phase pressure drop exist. Similarly, the two phase pressure fluctuations of such a system have not been investigated thoroughly in literature. This paper aims at extending our experimental knowledge of these issues.

### III. EXPERIMENTAL SETUP

To investigate the effect of the linear increase of the channel diameter two test sections have been made:

1. a stainless steel reference channel with a constant diameter of 0.6mm
2. a stainless steel conical channel with an inlet diameter of 0.6mm and an outlet diameter of 3mm

The theoretical friction reduction factor for a 5 time diameter increase is 0.083, and the momentum reduction factor is 0.001. Therefore, momentum induced pressure drops are neglected for the conical setup.

To investigate the effect of creating a gas bearing near the wall:

a conical channel with a porous wall: inlet diameter is 0.6mm and an outlet diameter is 3mm

#### A. Schematic Overview

Two measurement setups have been made to investigate the effect of channel widening and a third channel to investigate the effect of applying a gas bearing. A reference channel, of constant cross-section, and two conical channels have been utilized. All three have the same (heated) length of 50mm combined with an entrance length of 14.75mm results in a total length of 64.7mm, see Figs.2-4.

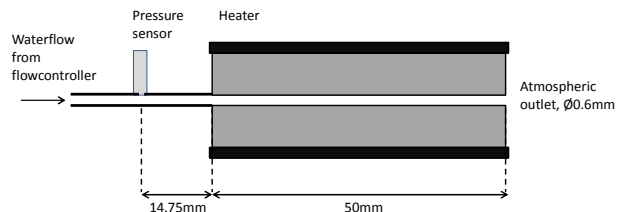


Fig. 2 Schematic drawing of the reference channel: Heated length 50mm, constant diameter 0.6mm

Demineralised water ( $\sim 293\text{K}$ ) flows from the flow controller past the differential pressure sensor, which measures the pressure difference between the upstream location and the ambient pressure. No special attention is given with respect to degassing the water. The measurements of the reference channel are done with the Honeywell 142PC05D (FullScaleRange=34475Pa, error= $\pm 0.5\%$ ) pressure transducer and the measurements of both conical channels are done with a Honeywell 164PC01D37 (FullScaleRange=2492Pa, error= $\pm 0.5\%$ ). This sensor is placed near the interchangeable heated channel, however still allowing the visual detection of the backflow. Boiling starts at the heated section. Therefore, in the heated section a two-phase flow occurs. This heated channel has an atmospheric outlet, which ensures that the pressure measured by the pressure sensor equals the two-phase pressure drop of the channel. For comparison reasons the length of both conical channels is exact the same as the reference channel, see Fig.3.

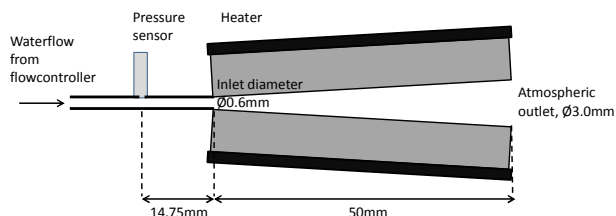


Fig. 3 Schematic drawing of the conical channel; the heated length equals the conical length: 50mm; the inlet diameter is 0.6mm and the outlet diameter is 3.0mm

For all three measurement setups the heat is supplied using a heating wire tightly spun around the outside wall. This heating wire allows the bearing gas to pass through the wall uniformly, see Fig. 4. A temperature sensor is placed 4mm after the inlet of the heated section and 0.8 mm from the channel interior wall. This temperature serves as an input for the electronic control system regulating the heat input. This temperature is kept constant during the measurement and is referred to as the wall temperature,  $T_{wall}$ . The water is supplied using a Bronkhorst flow controller (type mini-cori-flow, M12). The accuracy of the water flow controller is 0.2% of the actual value.

In order to supply the gas through the porous wall, an additional chamber is created around the heated channel. This gas tight chamber is fed by an Nitrogen supply using a Bronkhorst flow controller (type EL FLOW, F-201C), see Fig. 4. The accuracy of the Nitrogen flow controller 0.2% of the actual value plus 0.2ml/min i.e. 0.1% full scale.

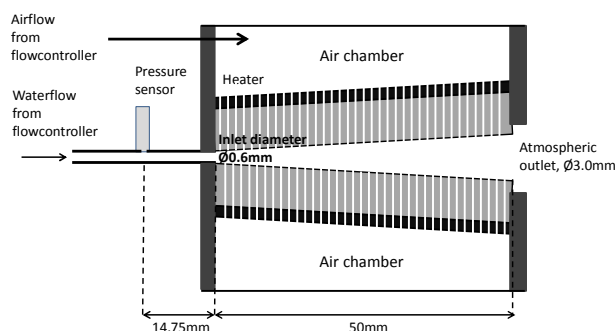


Fig. 4 Schematic drawing of the stainless steel conical channel with porous wall; the heated length equals the conical length: 50mm; the inlet diameter is 0.6mm and the outlet diameter is 3.0mm

The porous wall (SIKA-R 0.5AX) is made of small stainless steel particles sintered together. This results in Darcy-Forchheimer coefficients of  $0.08 \cdot 10^{-12} \text{m}^2$  and  $0.3 \cdot 10^{-7} \text{m}$  (i.e. a volume porosity  $\sim 21\%$ ) with a typical hole size of about 0.5 micro meter. The conical channel is made by Electrical Discharge Machining (wire EMD) in order to keep the pores open. Regular milling techniques would smear out the material and therefore create a closed wall.

#### B. Measurement Method

The measurements have been performed using the following procedure. First the heater is turned on and the wall is brought to the desired temperature. Typically, the wall temperature is set at approximately  $130^\circ\text{C}$ . For water this temperature is close to the critical heat flux temperature, which is  $126^\circ\text{C}$  for pool boiling. Next, the water is turned on and set to 1, 3, 5, 10, 15, 20, 30 and 40gr/hr. In case of the gas bearing experiments first a constant gas chamber pressure was set resulting to a defined Nitrogen supply ( $\sim 5$ ,  $\sim 10$ ,  $\sim 20$ ,  $\sim 40$ ,  $\sim 100$ ,  $\sim 150 \text{ml/min}$ ) before turning on the water flow. After a system stabilizing period of about 2 minutes, the pressure sensor is logged (read-out frequency 4Hz, or 1000Hz) for at least 2-5 minutes.

These data are used to obtain the average pressure drop and its variations. It is ensured that no gaseous phase is present in the tubing from channel to the sensor. The measurements for all three channels have been repeated, after pulling apart and reconstructing the entire measurement setup. The results did not change significantly ( $< 10\%$ ). Similarly, the readout frequency did not significantly affect the mean pressure drop results, nor the statistical values representing the pressure fluctuations.

## IV. RESULTS AND DISCUSSION

#### A. Results

The pressure drop signal varies in time due to boiling, see Fig. 5. The pressure fluctuations are represented by the standard deviation,  $\sigma$ , of the measured pressure drop.

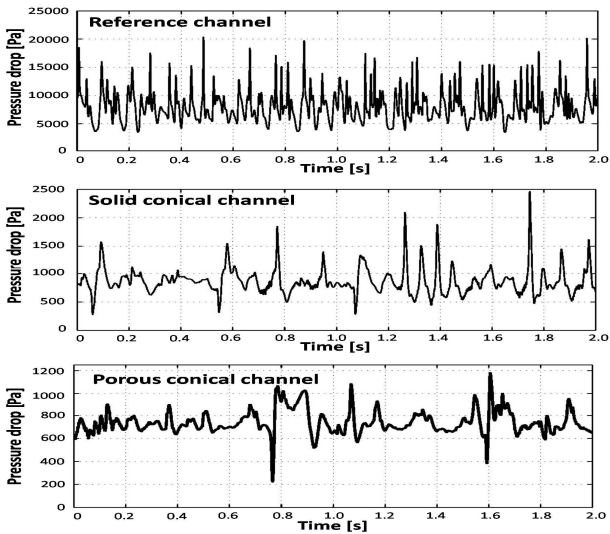


Fig. 5 Measured pressure drop as a function of time of the three boiling channels. Water supply flow 40gr/hr, temperature controlled at 130°C

Fig. 6 shows the measured average pressure drop for the reference channel and both conical channels for various water flow rates. The typical measurement reproduction for the average pressure drop for the straight channel is within 5%. The data reproduction of the average pressure drop for the two conical channels is about 5-10%. The pressure drop over the adiabatic liquid phase supply channel between the pressure sensor and the heated part is small as compared to the total pressure drop. At 40gr/hr, for example, this pressure drop is about 50 Pa.

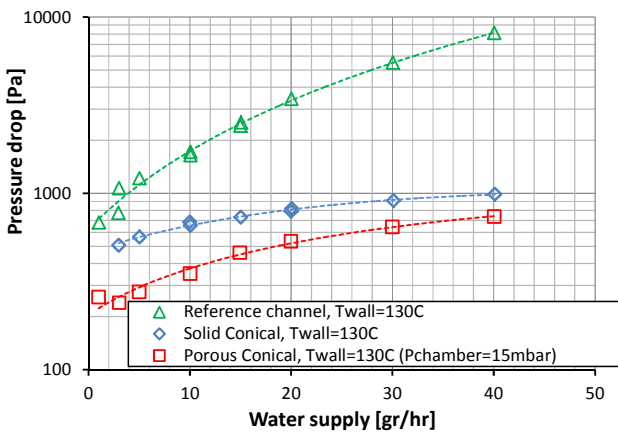


Fig. 6 Total measured pressure drop results for all three channels. Temperature controlled at 130°C

Altering the channel geometry from a straight channel to a conical channel reduces the total pressure drop by a factor 2 at low flow rates, to a factor 8 at high flow rates. This corresponds to the theoretical values obtained for conical channels with a diameter ratio,  $\alpha$ , varying from 1.5 to 4.5. The

porous wall conical channel reduces the pressure drop again by a factor 2 to 1.5 with respect to the solid conical channel. However, Fig. 6 shows as well that all curves have a certain offset going to zero water supply flow. If these zero-flow offsets are subtracted, the gas bearing does not have a significant influence on the total pressure drop compared to the solid conical measurement.

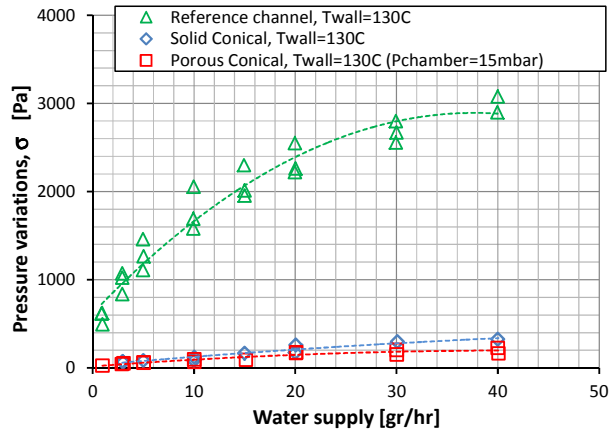


Fig. 7 Pressure fluctuations as quantified by  $\sigma$ , the standard deviation of the measured pressure signal in the course of time. Temperature controlled at 130°C

Fig. 7 shows that all curves for the pressure variations tend to go through zero at zero-flow. The main pressure fluctuation reduction (about a factor of 10) is obtained by the conical shape of the channel. The porous wall conical channel shows that the pressure fluctuations are reduced by another factor 1.5.

All data shown for the porous channel are the averaged data obtained with the full range of Nitrogen supplies through the porous wall, 5 - 150ml/min. The influence of the Nitrogen flow rate is investigated. Fig 8 compares the total boiling pressure drops and the standard deviation levels for various Nitrogen flow rates.

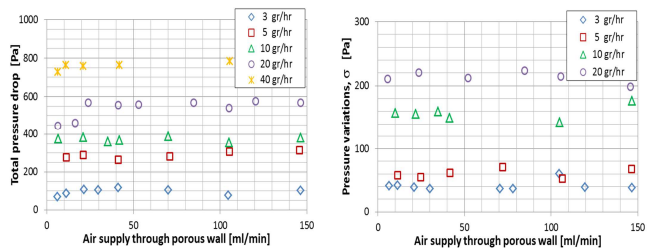


Fig. 8 Measured pressure drop (left) and standard deviation in pressure drop (right) as a function of the Nitrogen supplied through the porous wall

Fig. 8 shows no significant influence on both pressure drop and fluctuation level of varying the Nitrogen mass flow rate through the gas-chamber.

### B. Discussion

Pressure drop histories in Fig. 5 show upward spikes. As a general trend these spikes seem to scale with the total pressure drop. These spikes are believed to occur due to vapour bubble eruptions. As soon as a vapour bubble erupts it pushes the boiling mixture rapidly downstream, increasing for a short period its velocity. Since the (average) pressure drop scales with the mixture velocity, the pressure increase felt during such a bubble eruption scales with the average pressure drop as well. The pressure increase during an eruption is much more sudden in case of the straight reference channel than for the solid conical boiling channel, as is to be expected. Along with the reduction in absolute value of the pressure peaks, also the frequency of occurrence is reduced in both conical channels.

The gas supply through the heated wall in the porous channel significantly reduces the pressure fluctuations: by a factor of about 1.5. Although the measurement data are inconclusive about an actual average pressure drop reduction, the pressure variation data suggest that a gas bearing reduces the average pressure drop over a boiling channel as well. The reduction factor is independent of the amount of Nitrogen supplied. This is in agreement with the assumption that the Nitrogen lifts-off the water, at the least momentarily. As soon as a gas bearing is created shear stresses in the water near the wall decrease, almost regardless of the thickness of the gas layer.

### V. CONCLUSIONS

Pressure drops have been measured in three channel geometries: a straight reference channel, a conical channel and a conical channel with a porous wall through which Nitrogen is being supplied. From the pressure drop signal histories the average pressure drops and standard deviations have been estimated.

Experimental comparison shows that the measured reduction factor approaches a theoretically derived value. Pressure fluctuations are reduced by a factor of ten in the solid conical channel and a factor of 15 in the porous conical channel. This presumably leads to less backflow and therefore to a better flow control.

Reducing the average pressure drop reduces pressure fluctuations. Enlarging the diameter or the injection of gas through a porous wall promotes the operation stability of a once-through micro evaporator system.

### NOMENCLATURE

$a$	Numerical value depending on the channel geometry and liquid Reynolds number. For this study $a = 64$	[-]
$c$	Combined term depending on axial position	[N m]
$const$	Combined term of various constants	[N m]
$D$	Channel diameter	[m]
$D_h$	Hydraulic diameter	[m]
$D_i$	Inlet diameter	[m]
$D_o$	Outlet diameter	[m]
$G_{tot}$	Total mass flux	[kg m <sup>-2</sup> s <sup>-1</sup> ]

$l$	Axial position	[m]
$L$	Channel length	[m]
$\dot{m}_{tot}$	Total mass flow	[kg s <sup>-1</sup> ]
$n_1 n_2 n_3$	Empirical constants	[-]
$Re_{liq}$	Reynolds number based on the liquid mass flux	[-]
$x$	Vapour quality	[kg kg <sup>-1</sup> ]
$\alpha$	Diameter ratio	[-]
$\Delta P_{fric}$	Friction pressure drop	[Pa]
$\Delta P_{liq}$	Liquid pressure drop	[Pa]
$\Delta P_{mom}$	Momentum pressure drop	[Pa]
$\Delta P_{static}$	Hydrostatic pressure drop	[Pa]
$\Delta P_{tot}$	Total pressure drop	[Pa]
$\mu_{gas}$	Gas/Vapour viscosity	[Pa s]
$\mu_{liq}$	Liquid viscosity	[Pa s]
$\rho_{liq}$	Liquid density	[kg m <sup>-3</sup> ]
$\rho_{gas}$	Gas/Vapour density	[kg m <sup>-3</sup> ]
$\Phi_{CorrLiq}$	Two-phase flow pressure drop multiplier	[-]
$\chi^2$	Martinelli constant	[-]

### REFERENCES

- [1] C.M. Rops, L.F.G. Geers, J. Westerweel, "Explosive bubble growth during flow boiling in micro-channels," Proceedings of 5th European Thermal-Sciences Conference, Eindhoven, The Netherlands, 2008.
- [2] L. Zhang, E.N.Wang, K.E. Goodson, and T.W. Kenny "Phase change phenomena in silicon microchannels," International journal of heat and mass transfer, 48, pp. 1572-1582, 2005.
- [3] J.E. Kennedy, G.M. Roach Jr., M.F. Dowling, S.I. Abdel-Khalik, S.M. Ghiaasiaan, S.M. Jeter, Z.H. Quershi, "The onset of flow instability in uniformly heated horizontal microchannels," Journal of Heat Transfer, 122(1), p.p. 118-125, 2000.
- [4] K. Cornwell, P.A. Kew, "Boiling in small parallel channels," Proceedings of CEC Conference on Energy Efficiency in Process Technology, Athens, Greece, 1992.
- [5] S.G. Kandlikar, "Heat transfer mechanisms during flow boiling in microchannels," Journal of heat transfer, 126, pp. 8-16, 2004.
- [6] D. Brutin, L. Tadrist, "Pressure drop and heat transfer analysis of flow boiling in a minichannel: influence of the inlet condition on two-phase flow stability," International journal of heat and mass transfer, 47, pp. 2365-2377, 2004.
- [7] D. Brutin, F. Topin, L. Tadrist, "Experimental study of unsteady convective boiling in heated minichannels," International journal of heat and mass transfer, 46, pp. 2957-2965, 2003.
- [8] M. Ledinegg, "Instability of flow during natural and forced circulation," Wärme, 61(8), pp. 891-898, 1938.
- [9] P.S. Ramesh, K.E. Torrance, "Stability of boiling in porous media," International Journal of Heat and Mass Transfer 33(9), pp. 1895-1908, 1990.
- [10] P.S. Ramesh, K.E. Torrance, "Boiling in a porous layer heated from below: effects of natural convection and a moving liquid/two-phase interface," Journal of Fluid Mechanics 257, pp. 289-309, 1993.
- [11] D. Stemmelen, C. Moyne, A. Degiovanni, "Unstable boiling state in a porous medium," Institution of Chemical Engineers Symposium Series 2(129), pp. 1131-1137, 1992.
- [12] A. Sahli, C. Moyne, D. Stemmelen, "Boiling stability in a porous medium heated from below," Transport in porous media, 82(3), pp. 527-545, 2010.
- [13] W. Nakayama, T. Daikoku, T. Nakajima "Effects of pore diameters and system pressure on saturated pool nucleate boiling heat transfer from porous surfaces," Journal of Heat Transfer 104(2), p.p. 286-292, 1982.
- [14] S. Mori, K. Okuyama "Enhancement of the critical heat flux in saturated pool boiling using honeycomb porous media," International Journal of Multiphase Flow 35(10), p.p. 946-951, 2009.
- [15] S. Ghosh, T.K. Mandal, G. Das, P.K. Das "Review of oil water core annular flow," Renewable and Sustainable Energy Reviews 13(8), p.p. 1957-1965, 2009.
- [16] M.E. Nakla, D.C. Groeneveld, S.C. Cheng "Experimental study of inverted annular film boiling in a vertical tube cooled by R-134a" International Journal of Multiphase Flow, 37(1), pp. 67-75, 2011.

- [17] T. Takamasa, T. Hazuku, T. Hibiki "Experimental study of gas-liquid two-phase flow affected by wall surface wettability" International journal of heat and fluid flow, 29(6), pp. 1593-1602, 2008.
- [18] D. Huh, C.H. Kuo, J.B. Grotberg, S. Takayama "Gas-Liquid two-phase flow patterns in rectangular microchannels: effect of surface wetting properties," New journal of physics, 11, 2009.
- [19] J.H. Yan, T.S. Laker, S.M. Ghiaasiaan "Linear stability of inverted annular gas-liquid two-phase flow in capillaries" International journal of heat and fluid flow, 24(1), pp. 122-129, 2003.